Journal of Electronic Materials manuscript No.
(will be inserted by the editor)

Identification of Extended Defect Atomic Configurations in Silicon through Transmission Electron Microscopy Image Simulation

Iván Santos · Manuel Ruiz · María Aboy · Luis A. Marqués · Pedro López · Lourdes Pelaz

Received: date / Accepted: date

Abstract We used atomistic simulation tools to correlate experimental transmission electron microscopy images of extended defects in crystalline silicon with their structures at atomic level. Reliable atomic configurations of extended defects were generated using classical molecular dynamics simulations. High-resolution transmission electron microscopy (HRTEM) simulated images of obtained defects were compared to experimental images reported in the literature. We validated the developed procedure with the configurations proposed in the literature for {113} and {111} rod-like defects. We also proposed from our procedure configurations for {111} and {001} dislocation loops with simulated HRTEM images in excellent agreement with experimental images.

I. Santos · M. Ruiz · M. Aboy · L. A. Marqués · P. López · L. Pelaz

Dpto. Electricidad y Electrónica, E.T.S.I. Telecomunicación, Universidad de Valladolid, Paseo Belén 15, 47011 Valladolid, Spain

Corresponding author: I. Santos

E-mail: ivasan@tel.uva.es

Keywords extended defects · crystalline silicon · HRTEM · atomistic simulations

PACS 02.70.-c · 68.37.Og · 61.72.uf · 61.82.Fk

1 Introduction

Semiconductors are intentionally or unintentionally exposed to radiation of energetic particles during processing or during device operation. As energetic particles enter into a crystalline solid and interact with lattice atoms, point defects are generated. The accumulation and interaction of radiation-induced point defects lead to the formation of extended defects through an Ostwald ripening mechanism, which is driven by the reduction of defect formation energies [1]. In the particular case of crystalline Si (c-Si), Si interstitial extended defects are frequently formed after dopant implantation and thermal annealing processes used for the fabrication of junctions in electronic devices [2–8]. Extended defects can degrade the device performance by increasing leakage currents. They also act as reservoirs of Si self-interstitials, which are slowly released during subsequent thermal annealing treatment, causing dopant enhanced diffusion and electrical deactivation. Thus, the understanding of defect formation and dissolution mechanisms is essential for device optimization, and this involves the detailed knowledge of defect configurations [9, 10].

Among the extended defects observed in irradiated and annealed Si, {113} rod-like defects have attracted much attention as they are formed in conditions relevant for Si processing (10^{12}-10^{14} cm^{-2} implant doses, and thermal annealings up to 700-800°C [3, 10–12]). {113} rod-like defects have also been observed after high energy and high dose electron irradiation (2 MeV, $\sim 10^{22}$ cm^{-2} [13, 14]). Also,

Si samples irradiated by electrons (400 keV, $\sim 10^{23}$ cm^{-2} [5]) have shown rod-like defects in the {111} plane along the ⟨011⟩ direction. Planar dislocation loops in the {111} plane are more frequently observed after conventional Si processing for implant doses above 10^{14} cm^{-2} and temperature annealings above ~ 800°C [3, 10–12]. Just recently, dislocation loops in the {001} plane have been observed in implanted Si after partial melting nanosecond laser annealing [7].

These defects were experimentally visualized by transmission electron microscopy (TEM), which allows to elucidate their habit plane [2, 15]. High-resolution TEM (HRTEM) can be used to infer details of the atomic structure of extended defects as open spaces in the lattice or regions corresponding to atoms and bonds [4, 5]. However, it is not always possible to establish the exact positions of atoms in the defect from HRTEM images. Defect modeling can be a valuable complement to experimental imaging techniques for the unambiguous identification of the atomic defect structure. Classical molecular dynamics (CMD) simulations offer a good compromise to simulate at atomic level large extended defects, while accessing to long enough atom dynamics to explore the configurational landscape in the search of the most stable atomic configuration.

The aim of this work is to identify the atomic structure of extended defects in *c*-Si that are compatible with experimental TEM images by means of atomistic simulation tools.

2 Simulation details

We generated atomic configurations of extended defects using CMD simulations with LAMMPS code [16]. We used Tersoff potential on its third parametrization [17]

for describing interactions among Si atoms. This potential properly describes the properties of defects in *c*-Si, from Si self-interstitials [18] to extended defects [6, 19–21]. We used two different methods to obtain defect structures. In the first one, we placed Si self-interstitials at neighboring positions in the plane in which the defect under study is lying, and we performed a relaxation anneal so atoms could freely rearrange locally into the most favorable structure [19]. In the second method, we introduced isolated Si self-interstitials at random positions in a simulation cell, and we performed an intense annealing of the system so that Si interstitials could diffuse, interact and form more complex structures in any crystallographic plane [21]. The resulting defect structures, along with the surrounding crystal lattice, were introduced in the QSTEM software [22] to obtain the corresponding simulated HRTEM image.

3 Results and discussion

[Fig. 1 about here.]

The {113} rod-like defect has been widely studied in the past and its atomic structure was inferred by Takeda from HRTEM images [14]. More recent works have accurately established the atomic structure of not only linear {113} defects, but also structures that show steps, bends, or both, by direct comparison of defects obtained from CMD simulations with the atomic positions obtained from unprocessed high-angle annular dark field scanning TEM images [6, 20]. In our work, we obtained the atomic structure of {113} rod-like defects from an initial configuration generated by alternating Si interstitials and bond rearrangements in the {113} plane [19], as it is shown in Fig. 1.a. After relaxing this configuration with

CMD simulations, it naturally transformed into the structure of a {113} rod-like defect (shown in Fig. 1.b), with the typical E units (seven-membered rings at the boundaries which act as an interface between the {311} defect and perfect crystal), O units (eight-membered rings with no excess or deficit of atoms with respect to perfect lattice), and I units (two tiny rods of hexagonal Si containing interstitial $\langle 110 \rangle$ chains). The excellent agreement in the defective region between the simulated (Fig. 1.c) and the experimental (Fig. 1.d) HRTEM images validates the proposed structure for {113} rod-like defects, and our method to correlate experimental TEM images to atomistic structures. The irregular intensity distribution in the surrounding lattice observed in the experimental image was attributed to variations in the specimen thickness and defocus of the electron beam [14].

[Fig. 2 about here.]

While {113} rod-like defects are a favorable configuration for cluster sizes to about 200-300 interstitials, {111} loops are more stable for larger cluster sizes [12]. It has been postulated that {113} defects transforms into {111} loops when certain size is reached, being {111} rod-like defects the intermediate configurations in the transition between both type of defects [23]. Fedina and coworkers, who observed the elongated {111} defect directly by electron irradiation, proposed an atomistic model for {111} rod-like defects based on HRTEM images [5]. The configuration consisted of parallel Si interstitial chains elongated along the $\langle \overline{1}10 \rangle$ direction forming a regular sequence of double five- and single eight-member rings in the $\langle \overline{11}2 \rangle$ direction, as it is shown in Fig. 2.a. We replicated this structure and we used it as the starting configuration of a short relaxation CMD simulation. The simulated HRTEM image of the relaxed structure (Fig. 2.b) agrees well with

experimental images (Fig. 2.c), validating the proposed model for {111} rod-like defects.

[Fig. 3 about here.]

Nevertheless, our CMD simulations showed that the atomic structure of {111} rod-like defects is metastable and after annealing, it shrunk and transformed into a more stable configuration where Si interstitials formed a disk in an extra {111} plane, as it is shown in Fig. 3.a. {111} disk-like defects were also obtained from intense annealing CMD simulations where Si interstitials were randomly introduced in the sample [21]. The simulated HRTEM image of the obtained {111} disk-like defect is compatible with experimental HRTEM images of planar {111} dislocation loops in *c*-Si (Fig. 3). {111} dislocation loops are the more frequent defect observed experimentally after intense anneals of implanted Si [3, 10–12].

Although {001} loops are not thermodynamically favorable compared to {111} dislocation loops in *c*-Si, they were recently observed after partial melting nanosecond laser annealing of Si [7]. Defects on the {001} plane were also observed in deuteron irradiated Ge by Takeda and coworkers [4, 24]. They proposed a possible model for defects in the {001} plane consisting of a sequence of tetra-interstitials in the Arai configuration [25], as shown in Fig. 4.a. Nevertheless, bright spots associated to eight members rings in Takeda's model are absent in the experimental HRTEM image represented in Fig. 4.b. We used Takeda's structure as the starting configuration of annealing CMD simulations to obtain alternative structures for defects in the {001} plane. The resulting structure after annealing consisted on an extra {001} plane (Fig. 4.c). This structure was also obtained from very high temperature annealing CMD simulations when Si interstitials were randomly intro-

duced in the sample [21]. The simulated HRTEM image of the obtained structure (Fig. 4.d) is in excellent agreement with the experimental image (Fig. 4.b).

[Fig. 4 about here.]

4 Conclusions

We used simulation tools to identify atomic configurations of extended defects in *c*-Si compatible with experimental HRTEM images. The developed procedure consists on the relaxation of defect structures using CMD simulations, and the simulation of the HRTEM images of obtained defects. While in some cases we considered initial structures on the habit plane of the sought extended defects, atom dynamics during CMD simulations allowed their evolution into more favorable ones. This methodology was validated by the models proposed in the literature for {113} and {111} rod-like defects. It also allowed us to propose configurations for {111} and {001} dislocation loops that have simulated HRTEM images in excellent agreement with experimental images. The good correspondence between generated defect structures and experimental HRTEM images demonstrates that CMD simulations with Tersoff empirical potential in its third parametrization provide reliable structures of extended defects in *c*-Si.

Acknowledgements This work has been supported by EU (FEDER) and the Spanish Ministerio de Ciencia e Innovación under Project No. TEC2014-60694-P, and by the Junta de Castilla y León under Project No. VA331U14.

References

1. A. Claverie, B. Colombeau, F. Cristiano, A. Altibelli, C. Bonafos, Nucl. Instrum. Methods Phys. Res. B **186**, 281 (2002)
2. B. de Mauduit, L. Laânab, C. Bergaud, M.M. Faye, A. Martinez, A. Claverie, Nucl. Instrum. Methods Phys. Res. B **84**, 190 (1994)
3. P.A. Stolk, H.J. Gossmann, D.J. Eaglesham, D.C. Jacobson, C.S. Rafferty, G.H. Gilmer, M. Jaraíz, J.M. Poate, H.S. Luftman, T.E. Haynes, J. Appl. Phys. **81**, 6031 (1997)
4. S. Takeda, Microsc. Res. Tech. **40**, 313 (1998)
5. L. Fedina, A. Gutakovskii, A. Aseev, J.V. Landuyt, J. Vanhellemont, Philos. Mag A **77**, 423 (1998)
6. K.J. Dudeck, L.A. Marqués, A.P. Knights, R.M. Gwilliam, G.A. Botton, Phys. Rev. Lett. **110**, 166102 (2013)
7. Y. Qiu, F. Cristiano, K. Huet, F. Mazzamuto, G. Fisicaro, A. La Magna, M. Quillec, N. Cherkashin, H. Wang, S. Duguay, D. Blavette, Nano Letters **14**, 1769 (2014)
8. A. Claverie, N. Cherkashin, Nucl. Instrum. Methods Phys. Res. B **374**, 82 (2016)
9. L. Pelaz, L.A. Marqués, M. Aboy, P. López, I. Santos, Eur. Phys. J. B **72**, 323 (2009)
10. M. Aboy, I. Santos, L. Pelaz, L.A. Marqués, P. López, J. Comput. Electron. **13**, 40 (2014)
11. F. Cristiano, J. Grisolia, B. Colombeau, M. Omri, B. de Mauduit, A. Claverie, L.F. Giles, N.E.B. Cowern, J. Appl. Phys. **87**, 8420 (2000)

12. F. Cristiano, N. Cherkashin, X. Hebras, P. Calvo, Y. Lamrani, E. Scheid, B. de Mauduit, B. Colombeau, W. Lerch, S. Paul, A. Claverie, Nucl. Instrum. Methods Phys. Res. B **216**, 46 (2004)
13. S. Takeda, S. Muto, M. Hirata, Jpn. J. Appl. Phys. **29**, L1698 (1990)
14. S. Takeda, Jpn. J. Appl. Phys. **30**, L639 (1991)
15. G.Z. Pan, K.N. Tu, J. Appl. Phys. **82**, 601 (1997)
16. S. Plimpton, J. Comp. Phys. **117**, 1 (1995). `http://lammps.sandia.gov`
17. J. Tersoff, Phys. Rev. B **38**, 9902 (1988)
18. L.A. Marqués, L. Pelaz, P. Castrillo, J. Barbolla, Phys. Rev. B **71**, 085204 (2005)
19. L.A. Marqués, L. Pelaz, I. Santos, P. López, M. Aboy, Phys. Rev. B **78**, 193201 (2008)
20. L.A. Marqués, M. Aboy, K.J. Dudeck, G.A. Botton, A.P. Knights, R.M. Gwilliam, J. Appl. Phys. **115**, 143514 (2014)
21. L.A. Marqués, M. Aboy, M. Ruiz, I. Santos, P. López, L. Pelaz, Mater. Sci. Semicond. Process. **42**, 235 (2016)
22. QSTEM: Quantitative TEM/STEM Simulations, `http://qstem.org`
23. S. Boninelli, N. Cherkashin, A. Claverie, F. Cristiano, Appl. Phys. Lett. **89**, 161904 (2006)
24. S. Muto, S. Takeda, Philos. Mag. Lett. **72**, 99 (1995)
25. N. Arai, S. Takeda, M. Kohyama, Phys. Rev. Lett. **78**, 4265 (1997)

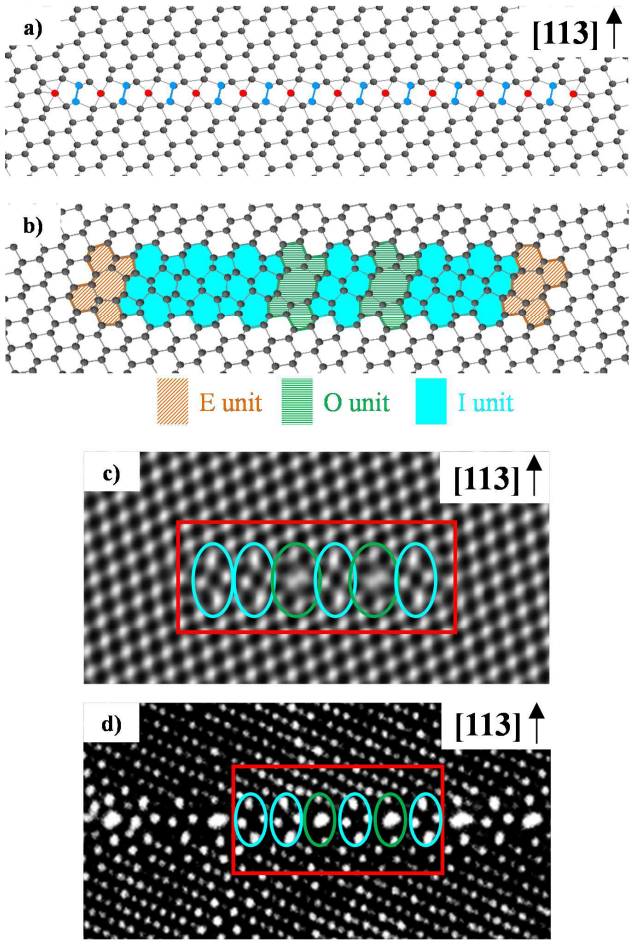

Fig. 1 (a) Atomic structure of {113} defect precursor, (b) atomic structure after CMD annealing, (c) simulated (based on Fig. 1.b) and (d) experimental (from Ref. [14], Copyright (1991) The Japan Society of Applied Physics) HRTEM images. Circles in (c) and (d) are to guide the eye.

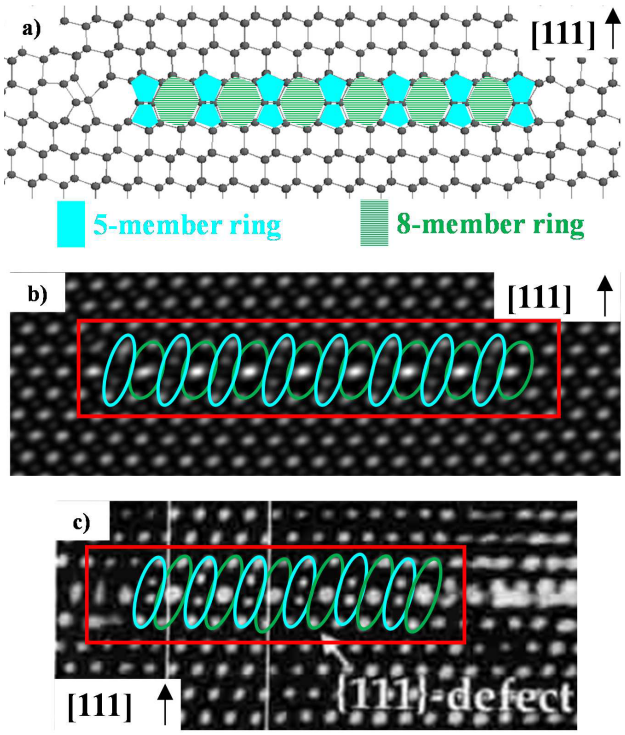

Fig. 2 (a) Atomic model for {111} rod-like defects proposed by Fedida [5]. (b) Simulated (based on Fig. 2.a) and (c) experimental (from Ref. [5], Copyright (1998) Taylor & Francis Ltd `http://www.tandfonline.com/`) HRTEM images of {111} rod-like defects. Circles in (b) and (c) are to guide the eye.

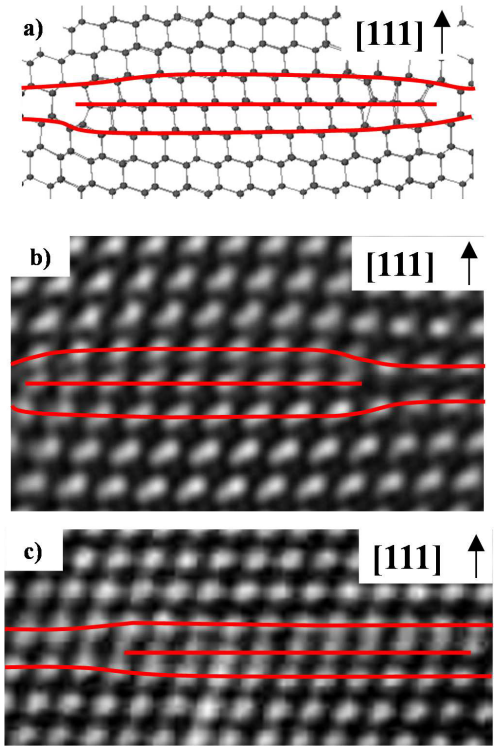

Fig. 3 (a) Atomic structure obtained after the annealing of the structure shown in Fig. 2.a. (b) Simulated (based on Fig. 3.a) and (c) experimental (from Ref. [5], Copyright (1998) Taylor & Francis Ltd `http://www.tandfonline.com/`) HRTEM images of {111} loops. Lines in (b) and (c) are to guide the eye.

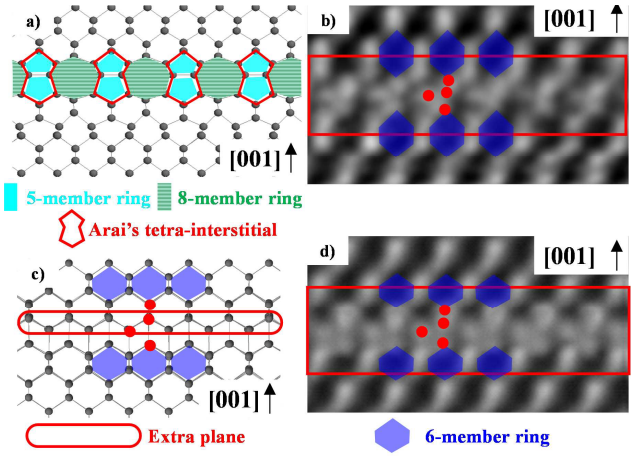

Fig. 4 a) Atomic structure of {001} defects proposed by Takeda [4], (b) experimental HRTEM image of {001} loops in Si (adapted with permission from Ref. [7]. Copyright (2014) American Chemical Society), (c) atomic structure obtained after the annealing of the structure shown in Fig. 4.a, and (d) simulated (based on Fig. 4.c) HRTEM image. Areas and dots are to guide the eye.